

# Transient Analysis of Electromagnetic Scattering using Marching-on-in-Order Time-Domain Integral Equation Method with Curvilinear RWG Basis Functions

Quan-quan Wang, Chao Yan, Yi-fei Shi, Da-zhi Ding, and Ru-shan Chen

Department of Communication Engineering  
Nanjing University of Science and Technology, Nanjing 210094, Jiangsu, China  
eeqqwang@gmail.com, eechenrs@mail.njust.edu.cn

**Abstract** — In this paper, a modified marching-on-in-order time-domain integral equation method is utilized to analyze transient electromagnetic scattering from arbitrarily shaped objects. The spatial and temporal testing procedures are separate, and both of them are performed with the Galerkin's method. The curvilinear RWG basis functions are used as spatial basis functions with curved triangular patch modeling. It gives a remarkable reduction to the number of unknowns, also the memory requirement and CPU time, without sacrificing the accuracy. The use of the weighted Laguerre polynomials as temporal basis functions ensures an absolutely stable solution even in late time. Several numerical results, including the single ogive and NASA almond, are given to demonstrate the accuracy and efficiency of the proposed method.

**Index Terms** — Curvilinear RWG basis functions, Laguerre polynomials, marching-on-in-order time-domain integral equation, transient scattering.

## I. INTRODUCTION

Accurate and efficient transient simulation has drawn great interest in the past decades for its important applications in the ultra wide band (UWB) technology, electromagnetic compatibility (EMC), radar imaging, etc. Numerical techniques in time domain falls mainly within the scope of the finite difference time-domain (FDTD) [1], the time-domain finite element method (TD-FEM) [2], and the time-domain integral equation (TDIE) [3], which can overcome the drawbacks encountered in the partial differential equation (PDE) methods.

The most popular method to solve TDIE is the marching-on-in-time (MOT) procedure [4], but it may suffer from late-time oscillation and inaccuracy. Some progresses seem to eliminate the drawback [5, 6].

In the realm of the integral equation method, the RWG basis function defined over the planar triangular patches was proposed to model the behavior of the induced surface current [7, 8]. Afterwards, the curvilinear counterpart with curved triangular patch modeling was developed, and much less unknowns are required without a loss of accuracy [9, 10].

References [11-13] used the curvilinear RWG (CRWG) basis functions and other techniques to analyze transient scattering based on the time-domain magnetic field integral equation (TD-MFIE) with MOT procedure. For closed bodies, because using the time-domain electric field integral equation (TD-EFIE) or TD-MFIE alone would lead to wrong results near the resonant frequencies, the time-domain combined field integral equation (TD-CFIE) is preferred [14].

Recently, the marching-on-in-order (MOO) TDIE solver with weighted Laguerre polynomials as temporal basis functions was introduced, which can obtain unconditionally stable solution [15-18]. In this scheme, accurate results near the resonant frequencies can be ensured with only TD-EFIE or TD-MFIE [18]. However, the conventional MOO TDIE method is not efficient in terms of RAM and CPU time. To circumvent the bottleneck, in this paper CRWG basis functions are utilized with MOO TD-EFIE to analyze the electromagnetic scattering from conducting objects.

This paper is organized as follows. Section II presents the formulation of MOO TD-EFIE and the CRWG basis functions. This is followed, in Section III, by giving several numerical results to demonstrate the accuracy and efficiency of the proposed method. The conclusion is drawn in Section IV.

## II. FORMULATION

### A. MOO TD-EFIE

With the boundary condition on the surface of the conducting scatterers, the time-domain electric field equation (TD-EFIE) is

$$\mathbf{E}^i(\mathbf{r}, t)|_{\tan} = \frac{1}{4\pi} \left[ \mu_0 \int \frac{\dot{\mathbf{J}}(\mathbf{r}', t - \Delta t_R)}{R} dS' - \frac{\nabla}{\epsilon_0} \int \int_0^{t - \Delta t_R} \frac{\nabla' \cdot \mathbf{J}(\mathbf{r}', \tau)}{R} d\tau dS' \right] |_{\tan}, \quad (1)$$

where  $\mathbf{E}^i(\mathbf{r}, t)$  is the incident electric field,  $R = |\mathbf{r} - \mathbf{r}'|$  is the distance between the observation point  $\mathbf{r}$  and source point  $\mathbf{r}'$ ,  $\Delta t_R = R/c$ ,  $\dot{\mathbf{J}}$  is the first derivative of the electric surface current density  $\mathbf{J}$  with respect to time  $t$ ,  $c$ ,  $\mu_0$ , and  $\epsilon_0$  are light speed, permeability, and permittivity in free space, respectively.

$\mathbf{J}$  can be expanded using  $N$  spatial basis functions and  $M$  temporal basis functions as

$$\mathbf{J}(\mathbf{r}, t) = \sum_{n=1}^N \left( \sum_{j=0}^{M-1} J_{n,j} \varphi_j(\bar{t}) \right) \mathbf{f}_n(\mathbf{r}), \quad (2)$$

and  $\mathbf{f}_n(\mathbf{r})$  is the spatial basis function and specifically the CRWG in this paper.  $\varphi_j(\bar{t})$  is the temporal basis function, i.e. the weighted Laguerre polynomial, defined as

$$\varphi_j(\bar{t}) \triangleq e^{-st/2} L_j(st), \quad (3)$$

where  $s$  is a temporal scaling factor and  $L_j$  is the  $j$ -th order Laguerre polynomial with the form

$$L_j(t) = \frac{e^t}{j!} \frac{d^j}{dt^j} (t^j e^{-t}), \quad 0 \leq t < \infty. \quad (4)$$

The temporal derivative and integration terms in (1) are given as [17]

$$\begin{aligned} \dot{J}_n(t) &= s \sum_{j=0}^{\infty} \left( 0.5 J_{n,j} + \sum_{k=0}^{j-1} J_{n,k} \right) \varphi_j(\bar{t}) \\ &\triangleq s \sum_{j=0}^{\infty} J_{n,j}^D \varphi_j(\bar{t}) \end{aligned}, \quad (5)$$

$$\begin{aligned} \int_0^t J_n(\tau) d\tau &= \frac{2}{s} \sum_{j=0}^{\infty} \left( J_{n,j} + 2 \sum_{k=0}^{j-1} J_{n,k} (-1)^{j+k} \right) \varphi_j(\bar{t}) \\ &\triangleq \frac{2}{s} \sum_{j=0}^{\infty} J_{n,j}^I \varphi_j(\bar{t}) \end{aligned}, \quad (6)$$

After the spatial and temporal testing procedure with the Galerkin's method, for the  $i$ -th order case we obtain

$$\begin{aligned} &\left( s A_{mn} 0.5 J_{n,i} + \frac{2}{s} \Psi_{mn} J_{n,i} \right) e^{-\frac{s \Delta t_R}{2}} \\ &= \int_0^{\infty} V_m(t) \varphi_i(\bar{t}) dt - \\ &\sum_{j=0}^{i-1} \left\{ s A_{mn} J_{n,j}^D + \frac{2}{s} \Psi_{mn} J_{n,j}^I \right\} \varphi_{i,j}(s \Delta t_R) - \\ &\left[ s A_{mn} \sum_{k=0}^{i-1} J_{n,k} + \frac{2}{s} \Psi_{mn} \cdot 2 \sum_{k=0}^{i-1} J_{n,k} (-1)^{k+i} \right] e^{-\frac{s \Delta t_R}{2}} \end{aligned}, \quad (7)$$

where

$$\varphi_{i,j}(s \Delta t_R) = \varphi_{i-j}(s \Delta t_R) - \varphi_{i-j-1}(s \Delta t_R), \quad (8)$$

$$A_{mn} = \frac{\mu_0}{4\pi} \int \mathbf{f}_m(\mathbf{r}) \cdot \int \frac{\mathbf{f}_n(\mathbf{r}')}{R} dS' dS, \quad (9)$$

$$\Psi_{mn} = \frac{1}{4\pi \epsilon_0} \int \nabla \cdot \mathbf{f}_m(\mathbf{r}) \int \frac{\nabla' \cdot \mathbf{f}_n(\mathbf{r}')}{R} dS' dS, \quad (10)$$

$$V_m(t) = \int \mathbf{f}_m(\mathbf{r}) \cdot \mathbf{E}^i(\mathbf{r}, t) dS. \quad (11)$$

Rewrite (7) into a matrix equation

$$[\mathbf{Z}_{mn}^E][\mathbf{J}_{n,i}] = [\mathbf{V}_{m,i}^E] - [\mathbf{V}^{tE}_{m,i}], \quad (12)$$

where

$$\mathbf{Z}_{mn}^E = \left( s A_{mn} 0.5 + \frac{2}{s} \Psi_{mn} \right) e^{-\frac{s \Delta t_R}{2}}, \quad (13)$$

$$\mathbf{V}_{m,i}^E = \int_0^{\infty} V_m(t) \varphi_i(\bar{t}) dt, \quad (14)$$

$$\begin{aligned} \mathbf{V}^{tE}_{m,i} &= \sum_{j=0}^{i-1} \left\{ s A_{mn} J_{n,j}^D + \frac{2}{s} \Psi_{mn} J_{n,j}^I \right\} \varphi_{i,j}(s \Delta t_R) + \\ &\left[ s A_{mn} \sum_{k=0}^{i-1} J_{n,k} + \frac{2}{s} \Psi_{mn} \cdot 2 \sum_{k=0}^{i-1} J_{n,k} (-1)^{k+i} \right] e^{-\frac{s \Delta t_R}{2}}. \end{aligned} \quad (15)$$

We can solve the matrix equation recursively to get the temporal coefficients order by order. Then the surface current density can be obtained from (2).

## B. CRWG basis function

The CRWG basis functions are defined over curved triangular patches. Compared with planar triangular patches, the curved ones give a significant reduction to the mesh density, and hence the number of spatial unknowns, without a loss of the accuracy of the geometry modeling and the numerical solution.

As shown in Fig. 1, a curved triangular patch is defined by six nodes, and a position in the  $(\xi_1, \xi_2)$  parameter space is described by

$$\mathbf{r}(\xi_1, \xi_2) = \sum_{j=1}^6 \varphi_j(\xi_1, \xi_2) \mathbf{r}_j, \quad (16)$$

where  $\mathbf{r}_j$  is the Cartesian coordinate,  $\varphi_j(\xi_1, \xi_2)$  is the shape function with the form

$$\varphi_j(\xi_1, \xi_2) = \begin{cases} 2\xi_j(\xi_j - 1/2), & j=1,2,3 \\ 4\xi_{j-3}\xi_{j-5}, & j=4,5,6 \end{cases}, \quad (17)$$

and

$$\xi_1 + \xi_2 + \xi_3 = 1. \quad (18)$$

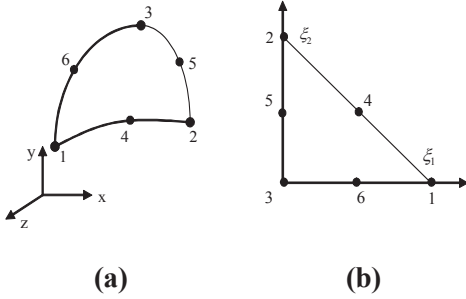


Fig. 1. (a) A curved triangular patch with six nodes in the Cartesian coordinate system, (b) The triangular patch in the  $(\xi_1, \xi_2)$  parametric space.

The CRWG basis function is defined as

$$\begin{cases} \mathbf{f}_1(\mathbf{r}) = \frac{\pm 1}{J} [\xi_2 \mathbf{I}_3 - (1 - \xi_1 - \xi_2) \mathbf{I}_2] \\ \mathbf{f}_2(\mathbf{r}) = \frac{\pm 1}{J} ((1 - \xi_1 - \xi_2) \mathbf{I}_1 - \xi_1 \mathbf{I}_3), \\ \mathbf{f}_3(\mathbf{r}) = \frac{\pm 1}{J} (\xi_1 \mathbf{I}_2 - \xi_2 \mathbf{I}_1) \end{cases}, \quad (19)$$

where

$$\mathbf{I}_1 = -\frac{\partial \mathbf{r}}{\partial \xi_2}, \quad \mathbf{I}_2 = \frac{\partial \mathbf{r}}{\partial \xi_1}, \quad \mathbf{I}_3 = \frac{\partial \mathbf{r}}{\partial \xi_2} - \frac{\partial \mathbf{r}}{\partial \xi_1}, \quad (20)$$

and  $J$  is the Jacobi factor

$$J(\xi_1, \xi_2) = \left| \frac{\partial \mathbf{r}}{\partial \xi_1} \times \frac{\partial \mathbf{r}}{\partial \xi_2} \right|. \quad (21)$$

The surface divergence of the CRWG basis function is

$$\nabla_s \cdot \mathbf{f}_\beta(\mathbf{r}) = \frac{\pm 2}{\sqrt{J}} \quad (\beta=1,2,3). \quad (22)$$

The differential tangent vector and normal surface element are given below, respectively,

$$d\mathbf{r} = \frac{\partial \mathbf{r}}{\partial \xi_1} d\xi_1 + \frac{\partial \mathbf{r}}{\partial \xi_2} d\xi_2, \quad (23)$$

$$d\mathbf{S} = \frac{\partial \mathbf{r}}{\partial \xi_1} \times \frac{\partial \mathbf{r}}{\partial \xi_2} d\xi_1 d\xi_2. \quad (24)$$

The surface normal unit vector is

$$\hat{\mathbf{n}}(\xi_1, \xi_2) = \frac{1}{\sqrt{g}} \frac{\partial \mathbf{r}}{\partial \xi_1} \times \frac{\partial \mathbf{r}}{\partial \xi_2}, \quad (25)$$

where

$$g = g_{11}g_{22} - g_{12}^2, \quad (26)$$

$$g_{ij} = \frac{\partial \mathbf{r}}{\partial \xi_i} \cdot \frac{\partial \mathbf{r}}{\partial \xi_j}. \quad (27)$$

## III. NUMERICAL EXAMPLES

This section gives several numerical results obtained using an implementation described above to validate the proposed method. All CPU times are taken on a 3.0GHz processor.

### A. Sphere

As the first example, we consider a metallic sphere centered at the origin with a radius of 0.5 meter. The problem is discretized into 219 CRWG basis functions and 50 temporal basis functions (i.e., the weighted Laguerre polynomials). The incident Gaussian pulse is with the form of

$$\mathbf{E}^i(\mathbf{r}, t) = \hat{\mathbf{x}} \frac{4}{\sqrt{\pi T}} e^{-\gamma^2}, \quad (28)$$

$$\gamma = \frac{4}{T} (t - t_0 - \mathbf{r} \cdot \hat{\mathbf{k}}/c), \quad (29)$$

where  $\hat{\mathbf{k}}$  is the unit vector in the direction of the wave propagation and is along  $-\hat{\mathbf{z}}$  direction in this example.  $t_0 = 12$  lm represents a time delay of the pulse peak from the time origin, and  $T = 8$  lm is the pulse width. In this work, we use lm as time unit, which is the short form of light meter. One light meter is the time taken by the electromagnetic wave to travel one meter in free space. This pulse has a frequency spectrum of 125 MHz. The scaling factor  $s$  is with the value of  $1.0 \times 10^9$ .

The  $\theta$  component of the backward far field response ( $\theta = 0^\circ$ ,  $\phi = 0^\circ$ ) from the sphere is shown in Fig. 2 (labeled C 219). For the sake of comparison, results obtained in Reference [18] (labeled Ref) and that via 795 conventional planar RWG (PRWG) basis functions (labeled P 795) are also shown. Good agreement can be observed.

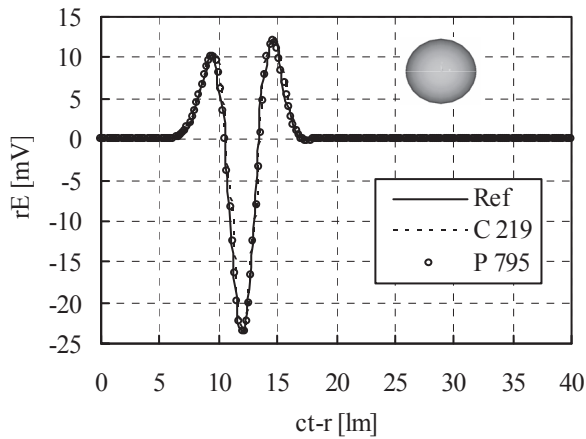


Fig. 2.  $\theta$  component of transient backward far field response from a sphere.

### B. Single ogive

Another example is a metallic single ogive. The analytical expression for this target is as follows:

for  $-1.27 \text{ m} < x < 1.27 \text{ m}$  and  $-\pi < \varphi < \pi$ , define

$$\begin{aligned} f(x) &= \sqrt{1 - \left(\frac{x}{5}\right)^2 \sin^2 22.62^\circ} - \cos 22.62^\circ \\ y &= \frac{f(x) \cos \varphi}{1 - \cos 22.62^\circ} \\ z &= \frac{f(x) \sin \varphi}{1 - \cos 22.62^\circ} \end{aligned} \quad (30)$$

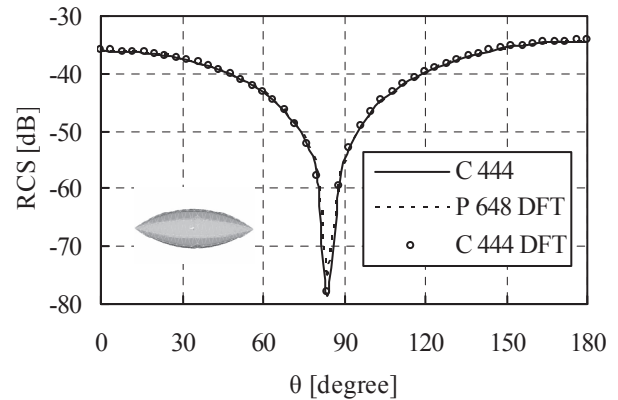
The incident wave used in this example is a modulated Gaussian pulse given by

$$\mathbf{E}^i(\mathbf{r}, t) = \hat{\mathbf{x}} \cos(2\pi f_0 \tau) \exp\left(-\frac{(\tau - t_p)^2}{2\sigma^2}\right), \quad (31)$$

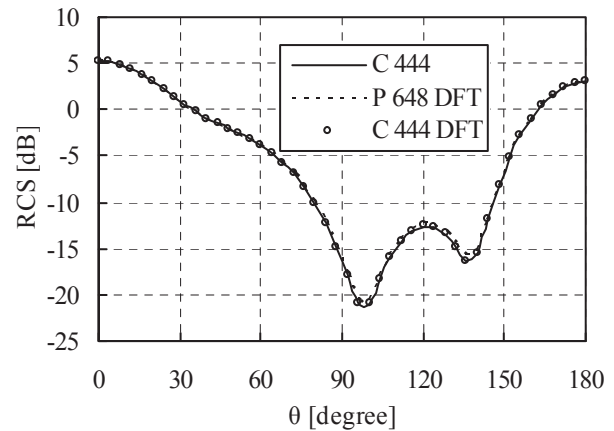
where the central frequency  $f_0$  is 160 MHz,  $\tau = t - \mathbf{r} \cdot \hat{\mathbf{k}}/c$ ,  $\hat{\mathbf{k}}$  is along  $-\hat{\mathbf{z}}$  direction,  $\sigma = 6/(2\pi f_{bw})$ ,  $t_p = 4.5\sigma$ , the bandwidth  $f_{bw}$  of the signal is 320MHz.

The problem is discretized into 444 CRWG basis functions and 100 temporal basis functions. The scaling factor  $s$  is with the value of  $1.5 \times 10^9$ .

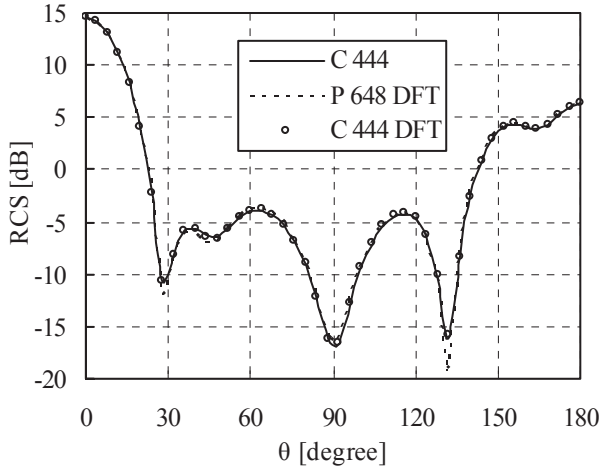
After the solution procedure in time domain, the far-field signals are Fourier transformed into the frequency domain and then the bistatic radar cross section (RCS) in  $\varphi = 0^\circ$  plane at several representative frequencies are calculated. These frequencies are chosen near the lowest, the middle and the highest frequency of the frequency band, and in this example they are 20 MHz, 160 MHz and 300 MHz. The results (labeled CRWG 444 DFT) are compared with those obtained via frequency domain MoM using 444 CRWGs (labeled C 444) and TD-EFIE using 648 PRWGs (labeled P 648 DFT) in Fig. 3. The results are in good agreement with each other. It's worth mentioning that 648 is the minimum number of PRWGs through exhaustive numerical experiments with increasing spatial unknowns.



(a)



(b)



(c)

Fig. 3. Bistatic RCS of the single ogive: (a) 20 MHz, (b) 160 MHz, and (c) 300 MHz.

**C. NASA almond**

A metallic NASA almond is referred to as the last structure. The mathematical description used for this target is as follows:

for  $-0.41667 < l < 0$  and  $-\pi < \varphi < \pi$ , define

$$x = dl \text{ m}$$

$$y = 0.193333d \sqrt{1 - \left(\frac{l}{0.416667}\right)^2} \cos \varphi, \quad (32)$$

$$z = 0.0644444d \sqrt{1 - \left(\frac{l}{0.416667}\right)^2} \sin \varphi$$

for  $0 < l < 0.58333$  and  $-\pi < \varphi < \pi$

$$x = dl \text{ m}$$

$$y = 4.83345d \left[ \sqrt{1 - \left(\frac{l}{2.08335}\right)^2} - 0.96 \right] \cos \varphi. \quad (33)$$

$$z = 1.61115d \left[ \sqrt{1 - \left(\frac{l}{2.08335}\right)^2} - 0.96 \right] \sin \varphi$$

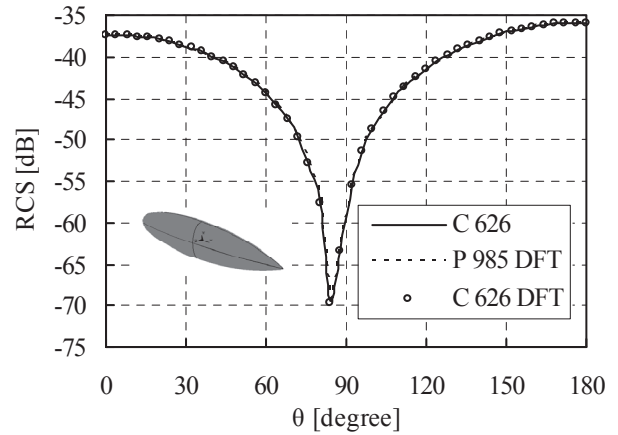
where  $d=2.52374 \text{ m}$ .

The incident wave used in this example is a modulated Gaussian pulse with the form of (31). The problem is discretized into 626 CRWG basis functions and 100 temporal basis functions. The central frequency of the incident modulated Gaussian pulse is 110 MHz and the frequency bandwidth is 220 MHz. The scaling factor  $s$  is with the value of  $1.5 \times 10^9$ . After a Fourier

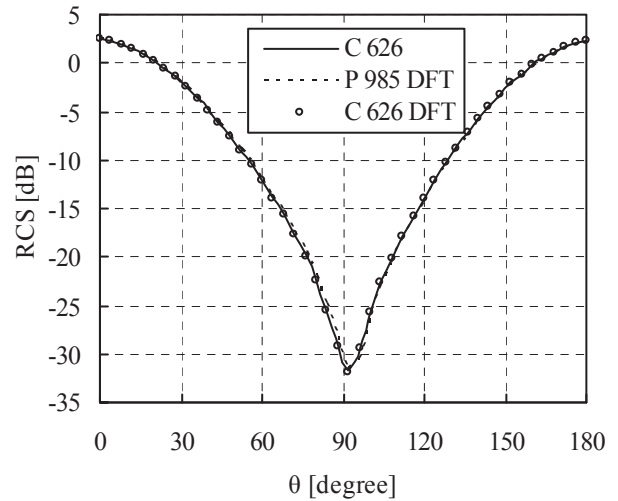
transform, the bistatic RCS in  $\varphi = 0^\circ$  plane at 20 MHz, 110 MHz and 200 MHz are given.

The result (labeled C 626 DFT) is compared with those obtained via frequency domain MoM using 626 CRWGs (labeled C 626) and TD-EFIE using 985 PRWGs (labeled P 985 DFT) in Fig. 4. 985 is found to be the minimum number of PRWGs for an almost indistinguishable result, which are more than that of the CRWGs.

The efficiency of the proposed method is further compared in Table 1. Considerable reduction to both memory requirement and total CPU time are achieved.



(a)



(b)



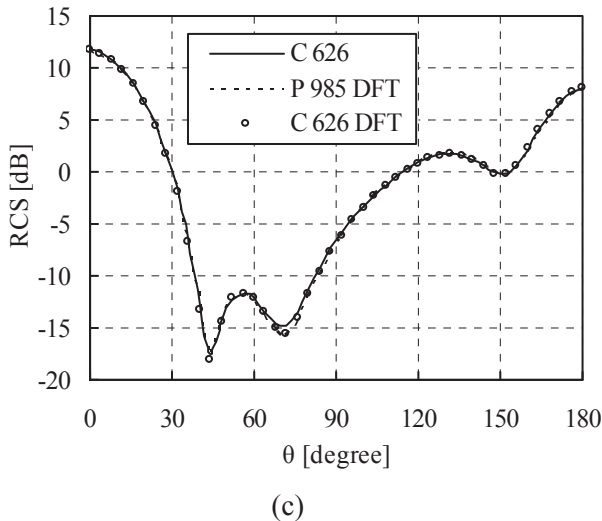


Fig. 4. Bistatic RCS of the NASA almond: (a) 20 MHz, (b) 110 MHz, and (c) 200 MHz.

Table 1: Comparison of memory requirement and total CPU time

		Geometries		
		Sphere	Ogive	Almond
Matrix Size	PRWG	795	648	985
	CRWG	219	444	626
RAM (MB)	PRWG	244	321	744
	CRWG	18	151	300
Total Time (s)	PRWG	275	754	1896
	CRWG	14	298	734

## VI. CONCLUSION

In this paper, the marching-on-in-order time-domain integral equation method with curvilinear RWG spatial basis functions is presented to analyze transient electromagnetic scattering from arbitrarily shaped objects. Stable solutions can be ensured, and the memory requirement and CPU time are reduced without sacrificing the accuracy.

## ACKNOWLEDGMENT

The authors would like to thank the editors and reviewers. The authors also appreciate the support of the Major State Basic Research Development Program of China (973 Program) under Grant No. 2009CB320201, the National Natural Science Foundation of China under Grant No. 60871013, and Jiangsu Natural Science Foundation under Grant No. BK2008048.

## REFERENCES

- [1] K. S. Yee, "Numerical Solution of Initial Boundary Value Problems Involving Maxwell's Equations in Isotropic Media," *IEEE Trans. Antennas Propagat.*, vol. AP-14, pp. 302-307, May 1966.
- [2] D. Jiao, J. M. Jin, E. Michielssen, and D. J. Riley, "Time-Domain Finite-Element Simulation of Three-Dimensional Scattering and Radiation Problems using Perfectly Matched Layers," *IEEE Trans. Antennas Propagat.*, vol. 51, no. 2, pp. 296-305, Feb. 2003.
- [3] S. M. Rao and T. K. Sarkar, "Numerical Solution of Time Domain Integral Equations for Arbitrarily Shaped Conductor/Dielectric Composite Bodies," *IEEE Trans. Antennas Propagat.*, vol. 50, no. 12, pp. 1831-1837, Dec. 2002.
- [4] S. M. Rao and D. R. Wilton, "Transient Scattering by Conducting Surfaces of Arbitrary Shape," *IEEE Trans. Antennas Propagat.*, vol. 39, no. 1, pp. 56-61, Jan. 1991.
- [5] F. P. Andriulli, K. Cools, F. Olyslager, and E. Michielssen, "Time Domain Calderón Identities and their Application to the Integral Equation Analysis of Scattering by PEC Objects Part II: Stability," *IEEE Trans. Antennas Propagat.*, vol. 57, no. 8, pp. 2365-2375, Aug. 2009.
- [6] Y. F. Shi, M. Y. Xia, R. S. Chen, E. Michielssen, and M. Y. Lu, "Stable Electric Field TDIE Solvers Via Quasi-Exact Evaluation of MOT Matrix Elements," *IEEE Trans. Antennas Propagat.*, vol. 59, no. 2, pp. 574-585, Feb. 2011.
- [7] S. M. Rao, D. R. Wilton, and A. W. Glisson, "Electromagnetic Scattering by Surfaces of Arbitrary Shape," *IEEE Trans. Antennas Propagat.*, vol. AP-30, no. 3, pp. 409-418, May 1982.
- [8] G. K. Carvajal, D. J. Duque, and A. J. Zozaya, "RCS Estimation of 3D Metallic Targets using the Moment Method and Rao-Wilton-Glisson Basis Functions," *Applied Computational Electromagnetic Society (ACES) Journal*, vol. 24, no. 5, pp. 487-492, Oct. 2009.
- [9] S. Wandzura, "Electric Current Basis Functions for Curved Surfaces,"

- Electromagn.*, vol. 12, no. 1, pp. 77-91, Jan.-Mar. 1992.
- [10] J. M. Song and W. C. Chew, "Moment Method Solutions using Parametric Geometry," *J. Electromagn. Waves Appl.*, vol. 9, no. 1/2, pp. 71-83, Jan.-Feb. 1995.
- [11] M. J. Bluck and S. P. Walker, "Time-Domain BIE Analysis of Large Three-Dimensional Electromagnetic Scattering Problem," *IEEE Trans. Antennas Propagat.*, vol. 45, no. 5, pp. 894-901, May 1997.
- [12] G. H. Zhang and M. Y. Xia, "An Enhanced TDIE Solver using Causal-Delayed Temporal Basis Functions and Curvilinear RWG Spatial Basis Functions," *Proc. Asia-Pacific Microwave Conf.*, Singapore, pp. 810-813, Dec. 2009.
- [13] S. W. Huang, G. H. Zhang, M. Y. Xia, and C. H. Chan, "Numerical Analysis of Scattering by Dielectric Random Rough Surfaces using Modified SMCG Scheme and Curvilinear RWG Basis Functions," *IEEE Trans. Antennas Propagat.*, vol. 57, no. 10, pp. 3392-3397, Oct. 2009.
- [14] G. H. Zhang and M. Y. Xia, "Time Domain Integral Equation Solvers using Curvilinear RWG Spatial Basis Functions and Quadratic B-Spline Temporal Basis Functions," *Proc. Asia-Pacific Microwave Conf.*, Hongkong, pp. 1-4, Dec. 2008.
- [15] B. H. Jung, Y. S. Chung, M. T. Yuan, and T. K. Sarkar, "Analysis of Transient Scattering from Conductors using Laguerre Polynomials as Temporal Basis Functions," *Applied Computational Electromagnetic Society (ACES) Journal*, vol. 19, no. 2, pp. 84-92, Jul. 2004.
- [16] Y. S. Chung, T. K. Sarkar, B. H. Jung, M. Salazar-Palma, Z. Ji, S.M. Jang, and K.J. Kim, "Solution of Time Domain Electric Field Integral Equation using the Laguerre Polynomials," *IEEE Trans. Antennas Propagat.*, vol. 52, no. 9, pp. 2319-2328, Sep. 2004.
- [17] Y. S. Chung, Y. J. Lee, J. H. So, J. Y. Kim, C. Y. Cheon, B. J. Lee, and T. K. Sarkar, "A Stable Solution of Time Domain Electric Field Integral Equation using Weighted Laguerre Polynomials," *Microwave Opt. Technol. Lett.*, vol. 49, no. 11, pp. 2789-2793, Nov. 2007.
- [18] B. H. Jung, Y. S. Chung, and T. K. Sarkar, "Time-Domain EFIE, MFIE, and CFIE Formulations using Laguerre Polynomials as Temporal Basis Functions for the Analysis of Transient Scattering from Arbitrary Shaped Conducting Structures," *Prog. Electromagn. Res.*, vol. 39, pp. 1-45, 2003.



**Quan-quan Wang** received the B.S. degree in Communication Engineering from Nanjing University of Science and Technology (NUST), China, in 2006.

He is currently working towards the Ph.D. degree in Electromagnetic Fields and Microwave Technology at NUST. His research interests include transient EM scattering and TDIE method.



**Chao Yan** received the B.S. degree in Electronic Information Engineering from Heilongjiang Institute of Science and Technology, China, in 2007, and the M.S. degree in Electromagnetic Fields and Microwave Technology from Nanjing University of Science and Technology, China, in 2010, respectively.

He is now an engineer in State-Owned Xianfeng Machinery Factory. His research interests include transient analysis and antennas.



**Yi-fei Shi** received the B.S. degree in Electrical Engineering from Nanjing University of Technology, China, in 2004.

He is currently working towards the Ph.D. degree in Electromagnetic Fields and Microwave Technology at Nanjing University of Science and Technology, China. His research interests include TDIE and its fast methods.



**Da-zhi Ding** received the B.S. and Ph.D. degrees in Electromagnetic Fields and Microwave Technology from Nanjing University of Science and Technology (NUST),

China, in 2002 and 2007, respectively. During 2005, he was with the Center of Wireless Communication in the City University of Hong Kong, Hong Kong SAR, China, as a Research Assistant.

He is currently an Associate Professor of NUST. He is the author or coauthor of over 30 technical papers. His current research interests include CEM and antennas.



**Ru-shan Chen** received the B.S. and M.S. degrees in Electronics from Southeast University, China, in 1987 and 1990, respectively, and the Ph.D. degree from the Department of Electronic Engineering, City University of Hong Kong (CUHK), Hong Kong SAR, China, in 2001. In 1990, he joined the Department of Electronic Engineering, Nanjing University of Science and Technology (NUST), China. Since 1996, he has been a Visiting Scholar with the Department of Electronic Engineering, CUHK. In 1999, he was promoted Full Professor of NUST, and in 2007, he was appointed Head of the Department of Communication Engineering.

His research interests mainly include CEM and millimeter wave systems. He has authored or coauthored more than 200 papers, including over 140 papers in international journals. Dr. Chen is the recipient of the Foundation for China Distinguished Young Investigators in 2003. In 2008, he became a Chang-Jiang Professor under the Cheung Kong Scholar Program of China.